Korean J. Chem. Eng., 36(10), 1595-1603 (2019)
DOI: 10.1007/s11814-019-0373-0

pISSN: 0256-1115
eISSN: 1975-7220

Ultrasonic-assisted synthesis of *Populus alba* activated carbon for water defluorination: Application for real wastewater

Ziaeddin Bonyadi*, Ponnusamy Senthil Kumar, Rauf Foroutan***, Raheleh Kafaei****, Hossein Arfaeinia*****,******, Sima Farjadfard*******, and Bahman Ramavandi*****,******,†**

*Environmental Health Engineering Department, Faculty of Health, Mashhad University of Medical Sciences, Mashhad, Iran
**Department of Chemical Engineering, SSN College of Engineering, Chennai 603 110, India
***Young Researchers and Elite Club, Bushehr Branch, Islamic Azad University, Bushehr, Iran
****Student Research Committee, School of Public Health and Safety, Shahid Beheshti University of Medical Sciences, Tehran, Iran
*****Department of Environmental Health Engineering, Faculty of Health and Nutrition, Bushehr University of Medical Sciences, Bushehr, Iran
******Systems Environmental Health and Energy Research Center, The Persian Gulf Biomedical Sciences Research Institute, Bushehr University of Medical Sciences, Bushehr, Iran
*******Department of Environmental Engineering, Graduate School of the Environment and Energy, Science and Research Branch, Islamic Azad University, Tehran, Iran
(*Received 8 July 2019 • accepted 22 August 2019*)

Abstract−Efficient activated carbon was ultrasonically synthesized from the *Populus alba* tree, and fluoride ions were removed from samples of synthetic and real wastewaters. The effects of various parameters including pH (2-10), time (5-180 min), contaminant concentration (10-100 mg/L), sorbent dose (1-7 g/L), and co-existing ions on the fluoride removal using *Populus alba* activated carbon (PAAC) were revealed. The physico-chemical characteristics of PAAC were determined using SEM, FTIR, BET, XRD, and EDX mapping. The specific surface area and pore volume of the mesoporous PAAC were obtained as 707.39 m^2/g and 0.40 m^3/g. The study found that the maximum removal efficiency of fluoride (93.37%) occurred under the fluoride concentration of 10 mg/L, PAAC of 4 g/L, pH of 6, and contact time of 100 min. The isotherms and kinetics data could be suitably reflected by the Freundlich and the pseudo-second-order kinetic models, respectively. Langmuir maximum monolayer adsorption capacity of the ultrasonic-assisted PAAC was measured as 77.12 mg/g. Sorption of fluoride ions onto PAAC is feasible and an exothermic process. According to the field test, PAAC can significantly remove fluoride and other pollutants like BOD_5, COD, Ni, Co, and Pb from glass and shipyard wastewater samples.

Keywords: Fluoride, *Populus alba*, Defluorination, Kinetics, Shipyard Wastewater, Glass Wastewater

INTRODUCTION

Fluoride is an inorganic pollutant naturally found in the environment. Based on the World Health Organization (WHO), it is classified as one of the water contaminants. Various natural sources such as granite, basalt, syenite, and shale can release fluoride into the groundwater. Furthermore, the untreated effluents of different industries, like semiconductor manufacturing, electroplating, coal-fired power stations, beryllium extraction plants, brick and iron works, and aluminum smelters, can increase the fluoride level of water bodies. The effluent of the industries contains a fluoride concentration of 10 to 1,000 mg/L [1,2]. It is assessed that more than 200 million people worldwide are exposed to fluoride with a concentration higher than that recommended by WHO (0.5-1.5 mg/L) [3]. The dental decay of children occurs usually at a fluoride concentration much less than 0.5 mg/L. On the other hand, the concentration fluoride>1.5 mg/L would cause different diseases such as dental fluorosis, brittle bones, osteoporosis, infertility, arthritis, cancer, thyroid disorder, and brain damage [1]. It may also cause neurological degeneration, headaches, muscle fiber degeneration, excessive thirst, red blood cell deformation, depression, abdominal pain, gastrointestinal issues, reduced immunity, and urinary tract disorders [1]. Therefore, due to the health effects of fluoride, this pollutant must be removed from wastewaters before being discharged into the environment.

Various technologies, like reverse osmosis, nano-filtration, coagulation, electrochemical method, ion-exchange, and precipitation, have been used for eliminating fluoride. However, these methods have limitations, such as high capital and operating costs, the complication of the treatment process, and chemical precipitation [4,5]. The adsorption method is considered a successful process for the removal of different elements from aqueous environments due to its excellent characteristics such as profitability, availability, low cost, ease of operation, and high efficiency [6].

In previous researches, defluorination process was surveyed by various adsorbents like activated carbon obtained from KOH-treated

†To whom correspondence should be addressed.
E-mail: ramavandi_b@yahoo.com, b.ramavandi@bpums.ac.ir

jamun (*Syzygium cumini*) seed [7], metal ions impregnated activated charcoal [8], and *Citrus aurantifolia* fruits-based activated carbon [9], *Musa paradisiaca* activated carbon and *Coffea arabica* husk activated carbon [10], and *Cynodon dactylon*-based activated carbon [11]. The production of many of these adsorbents is challenging in terms of environment and safety since metals and hazardous materials (such as acids and alkalis) have been used in their manufacture. If the metals are released from the adsorbent, it contaminates the treated liquid. Therefore, researchers are looking for better ways to make adsorbents that do not have the above-mentioned problems. One facile and effective method for the synthesis of adsorbents is the use of ultrasonic waves. Ultrasonic waves can produce hydroxyl radical, which is effective in the generation of new adsorptive sites and develops adsorbent pores [12,13]. In the ultrasonic method, no byproducts such as released metals are introduced into the treated solution and no hazardous solutions (acid or alkali) are consumed. Although ultrasonic method has been used to make adsorbents such as zirconium impregnated activated carbon [14,15] and melamine-formaldehyde-tetraoxalyl-ethylene diamine covered activated carbon (MFT/AC) [16], it has not been used to synthesize activated carbon from the *Populus alba* tree.

Populus alba is a tall, fast-growing and wild deciduous tree belonging to the willow family. The adult tree has a rounded crown and can grow to 18-30 m. *P. alba* has a high capacity to adapt to stressful conditions; thus, it is widely distributed in various countries such as Spain, France, Italy, Slovenia, Croatia, Turkey, Syria, Lebanon, Egypt, Libya, Tunisia, Algeria, and Morocco [17,18]. This tree grows abundantly at the western regions of Iran [19]. Waste branches of *P. alba* are considered as excellent and efficient adsorbent because they include some polar functional groups like carbonylic, alcoholic, phenolic and carboxylic groups, which would be potentially involved in the fast adsorption process of pollutants [20].

In this study, *P. alba* activated carbon (PAAC) was prepared in the presence of ultrasonic waves and used for defluoridation of contaminated water. The effects of various parameters including contact time, adsorbent dosage, solution pH, and fluoride concentration, and competing ions on the water defluoridation efficiency were explored. The field capability of the PAAC was examined by treating two wastewater samples (shipyard and glass wastewaters). Adsorption kinetics and isotherm studies were also implemented. The searches performed by the authors on reputable scientific websites showed that ultrasonic-assisted synthesis of PAAC has not been used to adsorb fluoride.

EXPERIMENTAL

1. Materials

All chemicals and reagents used in this research, including sodium hydroxide (NaOH), hydrochloric acid (HCl), sodium fluoride (NaF), sodium nitrate ($NaNO_3$), sodium chloride (NaCl), sodium sulfate (Na_2SO_4), sodium bicarbonate ($NaHCO_3$), and sodium phosphate (Na_3PO_4) were of analytical grade and purchased from Sigma-Aldrich.

2. PAAC Preparation

The wasted branches of *P. alba* tree were collected from western Iran without any cost. The wasted branches were crushed and washed with tap water and then oven-dried at 110 °C for 24 h. The dried material was powdered to less than 50 meshes. The activated carbon was produced from *P. alba* tree using the ultrasonic-assisted method. The amount of 3.5 g of dried powder was immersed in 28 mL 0.1 M NaOH solution for 1 h under the constant ultrasonic power (37 kHz). The sonication would lead to fast mass transfer at the liquid-solid interface. Subsequently, the mixture was dried in an oven (110 °C for 3 h) for dehydration purpose. The sonicated mixture was then activated in an electric furnace (SLG1100-60, China) at 750 °C for 100 min under flowing nitrogen gas of 350 mL/min. The materials were washed with double distilled water until the pH became 7±0.2. Finally, the obtained material was dehydrated at 110 °C for 8 h to constant weight. The PAAC adsorbent was also prepared without ultrasonic waves to compare with the ultrasonic-assisted one.

3. Characteristic Measurements

The characterization of PAAC was determined using different techniques including Brunauer-Emmett-Teller (BET), X-ray diffraction (XRD), Fourier-transform infrared spectroscopy (FT-IR), energy dispersive X-ray (EDX), and scanning electron microscope (SEM). The FT-IR spectrometer (Broker victor 22) was utilized for determining the functional groups in the PAAC surface and the interaction between the existing functional groups and fluoride after the adsorption process. XRD analysis was carried out using CuK_{α} radiation (35 kV, λ=1.5048 Å) in the 2θ range of 10-90° at the scanning speed of 5°/min. The surface morphology of the PAAC adsorbent was investigated using the SEM method (MIRA3-FEG, TESCAN, Czech). The BET analysis (ASAP2020, Micromeritics Co.) was applied to determine the specific surface area of PAAC by nitrogen single-layer adsorption calculated as a function of relative pressure.

4. Design of Experiments

4-1. General Conditions

The variables of this study included fluoride concentration (10-100 mg/L), PAAC dose (1-7 g/L), pH (2-10), and contact time (5-180 min). All tests were performed in 250 mL Erlenmeyer containing 100 mL of the reaction solution. In the experiment, 0.1 M HCl or NaOH solutions were used to regulate pHs. The reaction solutions were stirred by a shaker-incubator (Parsazmagostar, Iran) at 250 rpm. At definite time intervals, the reaction solution was passed through filter paper (Whatman No. 42), and 10 mL of the filtrate was used to determine the fluoride content. The residual fluoride concentration of filtrate was measured at λ_{max} of 570 nm by SPADNS method using UV-visible spectrophotometer (HACH DR5000) as demonstrated in Standard Methods for the Examination of Water and Wastewater [1]. The sorption efficiency of fluoride ions was obtained by the following formula:

$$\text{Sorption}\ (\%) = \frac{C_0 - C}{C_0} \times 100 \quad (1)$$

where C_0 denotes the initial F^- content (mg/L) and C denotes the F^- content in the treated solution after a given time (mg/L).

The amount of fluoride adsorbed per unit PAAC (q_e, mg/g) was determined using the following formula:

$$q_e = \frac{(C_0 - C_e)}{m} \times V \quad (2)$$

where C_e denotes the equilibrium content of F^- (mg/L), m denotes the mass of the PAAC adsorbent (g), and V denotes the volume of the used solution (L).

All experiments are repeated three times (n=3), and average measurements along with standard deviation (±SD) are reported herein. A control sample (lacking PAAC sorbent) was also used to track the effect of changing conditions during the experiments.

The specific test conditions were as follows:

4-2. Effect of Fluoride Concentration (10-100 mg/L)

The effect of fluoride concentration on sorption efficiency was studied at the working solution temperature of 25 °C, PAAC dose of 4 g/L, pH of 6, and contact time of 100 min.

4-3. Effect of Contact Time (5-180 min)

The effect of contact time on the fluoride sorption was investigated at the working solution temperature of 25 °C, sorbent dose of 4 g/L, pH of 6, and F^- content of 10 mg/L.

4-4. Effect of pH (2-10)

The effect of pH on the sorption rate was surveyed at the working solution temperature of 25 °C, PAAC dose of 4 g/L, contact time of 100 min, and F^- content of 10 mg/L.

4-5. Effect of PAAC Dose (1-7 g/L)

The effect of PAAC dose was examined at conditions of solution temperature of 25 °C, F^- content of 10 mg/L, contact time of 100 min, and pH of 6.

4-6. Effect of Co-existing Anions

The effect of co-existing anions (chloride, nitrate, sulfate, bicarbonate, and phosphate) of fluoride sorption was examined at the working solution temperature of 25 °C, PAAC dose of 4 g/L, contact time of 100 min, F^- content of 10 mg/L, and pH of 6.

4-7. Thermodynamics Tests

For studying adsorption thermodynamics, 3 g/L of PAAC was added into 100 mL of reaction solutions with experimental factors of pH of 6, F^- content of 50 mg/L, contact time of 180 min, and temperature of 298.15-328.15 °K. The thermodynamics factors of ΔG^o (standard Gibb's free energy), ΔH^o (standard enthalpy), and ΔS^o (standard entropy) were calculated using the following equations:

$$\ln K_c = \frac{\Delta S^o}{R} - \frac{\Delta H^o}{R}\left(\frac{1}{T}\right) \tag{3}$$

$$\Delta G^o = \Delta H^o - T\Delta S^o \tag{4}$$

where K_c is the thermodynamic equilibrium constant, which is explained as the ratio of adsorbed concentration to residue concentration of fluoride at equilibrium state, T is the absolute temperature in Kelvin scale (K), and R represents the gas constant.

4-8. Kinetic Study

The study of sorption kinetics was carried out using various parameters including the PAAC dose of 3 g/L, F^- content of 10-100 mg/L, pH of 6, and contact times of 5-180 min. The well-known models of pseudo-first and pseudo-second-order were used to evaluate the kinetics of F^- adsorption onto PAAC [6].

The pseudo-first-order model is expressed as Eq. (5):

$$q_t = q_e(1-\exp(-k_1 t)) \tag{5}$$

where k_1 (min^{-1}) and q_t (mg/g) are the pseudo-first-order kinetic constant and the amount of F^- adsorption capacity of PAAC at any time, respectively.

The pseudo-second-order model is described as follows:

$$q_t = \frac{q_e^2 k_2 t}{1+q_e k_2 t} \tag{6}$$

where k_2 (g/mg/min) is the rate constant for the pseudo-second-order model.

4-9. Equilibrium Study

The adsorption isotherms were investigated in the following conditions: adsorbent dose of 4 g/L, fluoride concentration of 20 mg/L, pH of 6, and contact time 180 min. The experiments were conducted at a solution temperature of 25 °C. The Langmuir and Freundlich equations were used to study the sorption isotherms. The Langmuir isotherm is described as follows:

$$q_e = \frac{q_m K_L C_e}{1+(K_L C_e)} \tag{7}$$

where q_m (mg/g) and K_L (L/mg) are expressed as the maximum sorption capacity and the Langmuir equilibrium constant, respectively.

The linear form of the Freundlich model is presented according to the following formula:

$$q_e = K_F C_e^{1/n} \tag{8}$$

where K_F $(mg/g(L\cdot mg)^{1/n})$ and n reflect constants which linked to capacity and intensity of F^- sorption by PAAC, respectively [4].

4-10. Zero-point of Charge (pH_{zpc}) Determination

To determine pH_{zpc}, 100 mL of 0.01 M NaCl solution was poured in flasks and the pH of solutions was regulated to around 2, 4, 6, 8, 10, and 11. Then, 2.5 g/L PAAC was added into the solutions, mixed at the fixed speed of 250 rpm for 24 h, and filtrated by Whatman paper 42. Finally, the difference between the initial and final pH values or "ΔpH=pHi−pHf" was plotted versus pHi.

4-11. Treatment of Real Wastewater

To assess the practical feasibility of PAAC for removing fluoride from a complex matrix, two real samples of wastewater were obtained from a Glass factory and Shipyard factory. The tests were done under the optimal conditions (PAAC dose of 4 g/L and the contact time of 100 min). The initial F^- concentration and pH of the wastewater were not changed to the desired amount.

RESULTS AND DISCUSSION

1. Characterization

1-1. BET

The BET surface area of the fresh and used PAAC sorbent was indicated in Table 1. The results displayed that the BET value of PAAC after fluoride sorption was reduced. The value of BET surface area before and after defluoridation was obtained as 707.39 m^2/g and 659.03 m^2/g, respectively. The surface area of the used PAAC decreased, probably due to sorption of fluoride. The BET surface area of ultrasonic-assisted synthesis of *P. alba* activated carbon was higher than that of pyrolyzed jamun seed (13.67 m^2/g) [7] and *Cynodon dactylon*-based thermally activated carbon [11] but lower than the activated jamun seed (747.45 m^2/g) [7]. Further, the specific surface area of ultrasonic-assisted PAAC was about 25%

Table 1. BET surface properties of the fresh and used sorbent

Parameter	Fresh ultrasonic-assisted PAAC	Used ultrasonic-assisted PAAC	Fresh non-ultrasonic-assisted sorbent
Mean pore diameter	2.85 nm	2.42 nm	2.42 nm
Pores structure	Mesopores	Mesopores	Mesopores
Total pore volume (P/P0=0.981)	0.504 cm^3/g	0.400 cm^3/g	0.381 cm^3/g
BET surface area	707.39 m^2/g	659.03 m^2/g	561.34 m^2/g
BET C coefficient	765.10	732.83	-
pHpzc	6.8	-	-

higher than that of simple sorbent (PAAC without ultrasonic-assisted). This indicates the effectiveness of the ultrasonic wave method for preparing the sorbent. The BET C coefficient was greater than 100 for the PAAC sorbent. This larger value is roughly consistent with single-layer sorption capacity [21]. The mean pore diameter of the fresh sorbent was obtained as 2.85 nm, while that of the used one was 2.42 nm. Based on the IUPAC size classification, the PAAC sorbent is mesoporous. The sorption of fluoride onto the PAAC significantly decreased the total pore volume and the surface area. The pore volume of the fresh sorbent was 0.50 cm^3/g, while that of the used sorbent was reduced to 0.40 cm^3/g. This is probably due to the loading of fluoride ions on the surface of sorbent. As shown in Table 1, the point of zero charges (pH_{pzc}) of PAAC was discovered to occur at 6.8. The pHpzc factor plays an important role in the adsorption of anions or cations onto adsorbents. The cation sorption is desired if the pH of the solution is higher than pH_{pzc}, while the anion (like fluoride) sorption is desired if the working solution pH is less than pH_{pzc} [22].

1-2. XRD

The XRD pattern of fresh and used PAAC is presented in Fig. 1. The fresh and used PAAC show two broad peaks at 23° and 43°, corresponding to the (002) and (100) planes, respectively. These broad peaks probably indicate that the PAAC sample consists of microcrystalline graphite [23]. The peak at 2θ=59.95° might be due to impurities in the prepared adsorbent, such as the carbon-metal complex, which disappeared after the adsorption process [24].

1-3. FTIR

The FT-IR analysis for activated carbon produced from *P. alba* (PAAC) before and after the fluoride ion sorption is shown in Fig. 2. As seen, the peaks at 3,432 cm^{-1} and 2,920 cm^{-1} are linked to stretching vibrations of -OH or adsorbed H_2O molecules and C-H groups in the structure of PAAC, respectively [25-27]. The peaks in the range of 1,035-1,460 cm^{-1} and 1,628 cm^{-1} could be due to the stretching vibrations (as symmetric or asymmetric) of C=O and C-O [28]. The observed peaks at 669 cm^{-1} and 869 cm^{-1} are related to the vibrations of -CN and S=O, respectively [29]. Based on the results, the range of vibrations and the intensity of absorption peaks in the PAAC structure after the fluoride sorption were changed, which could be due to the functional groups- F^- interaction. For example, after fluoride sorption, the peaks related to -OH, C-H, C-O, and C=O changed to 3,436 cm^{-1}, 2,925 cm^{-1}, 1,624 cm^{-1}, and 1,439 cm^{-1}, respectively. In the fluoride adsorbed PAAC, the bands at 600-1,600 cm^{-1} shifted due to the electrostatic adsorption between the F^- ion and the adsorbent [30]. Therefore, these changes were indicating the effective attribution of these functional groups in the adsorption of fluoride.

1-4. SEM, EDX, and Map

SEM, EDX, and Map analysis were applied to investigate the surface morphology, the value of main elements, and elements distribution of fresh and used PAAC. The results are shown in Fig. 3. The SEM analysis showed that activated carbon produced from *Populus alba* had a rough surface with different pores (Fig. 3(a)). These pores can be effective in the adsorption of fluoride ions. According to Map and EDX images (Fig. 3(b), (c)), the values of C

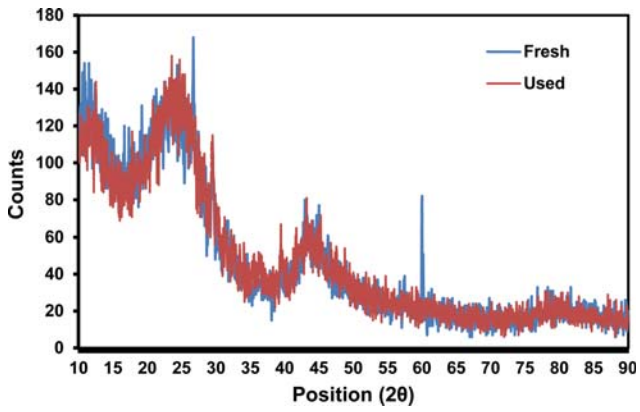

Fig. 1. XRD pattern of the fresh and used PAAC.

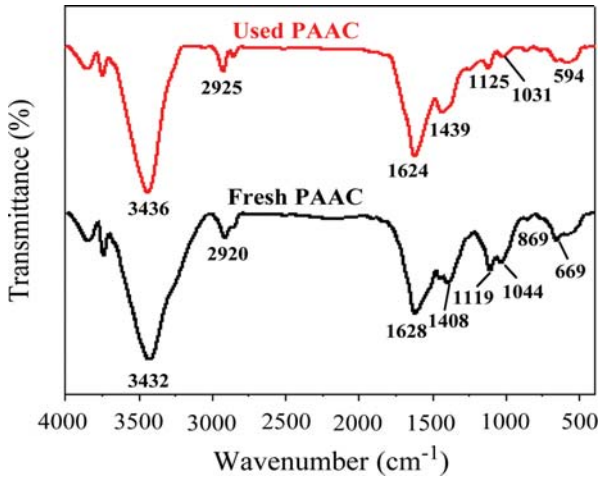

Fig. 2. FT-IR analysis for fresh and used PAAC.

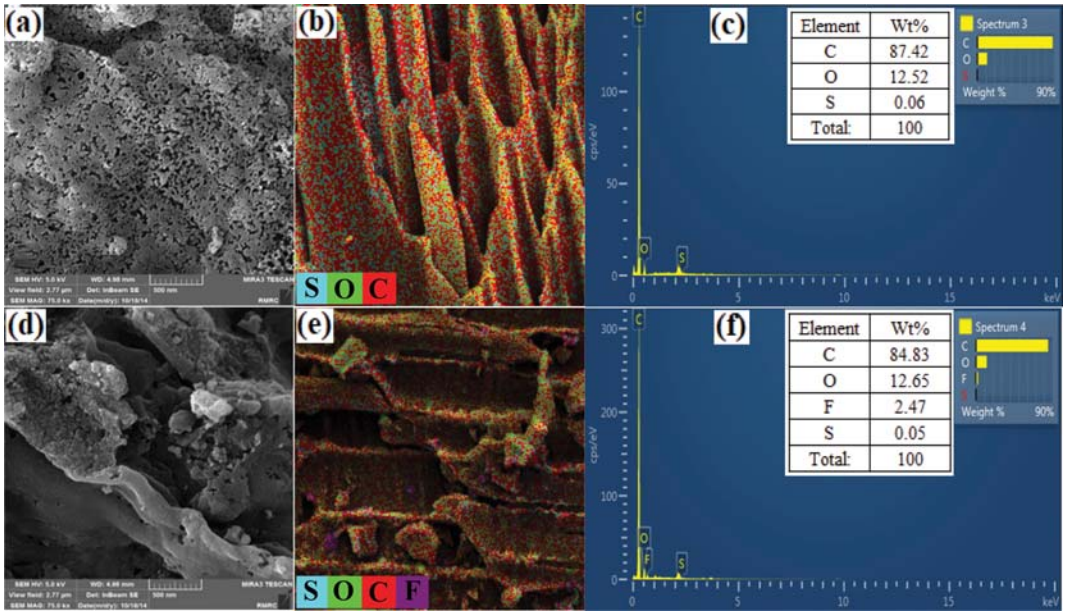

Fig. 3. Analysis of SEM, Map, and EDX for PAAC (a)-(c) before and (d)-(f) after the fluoride sorption.

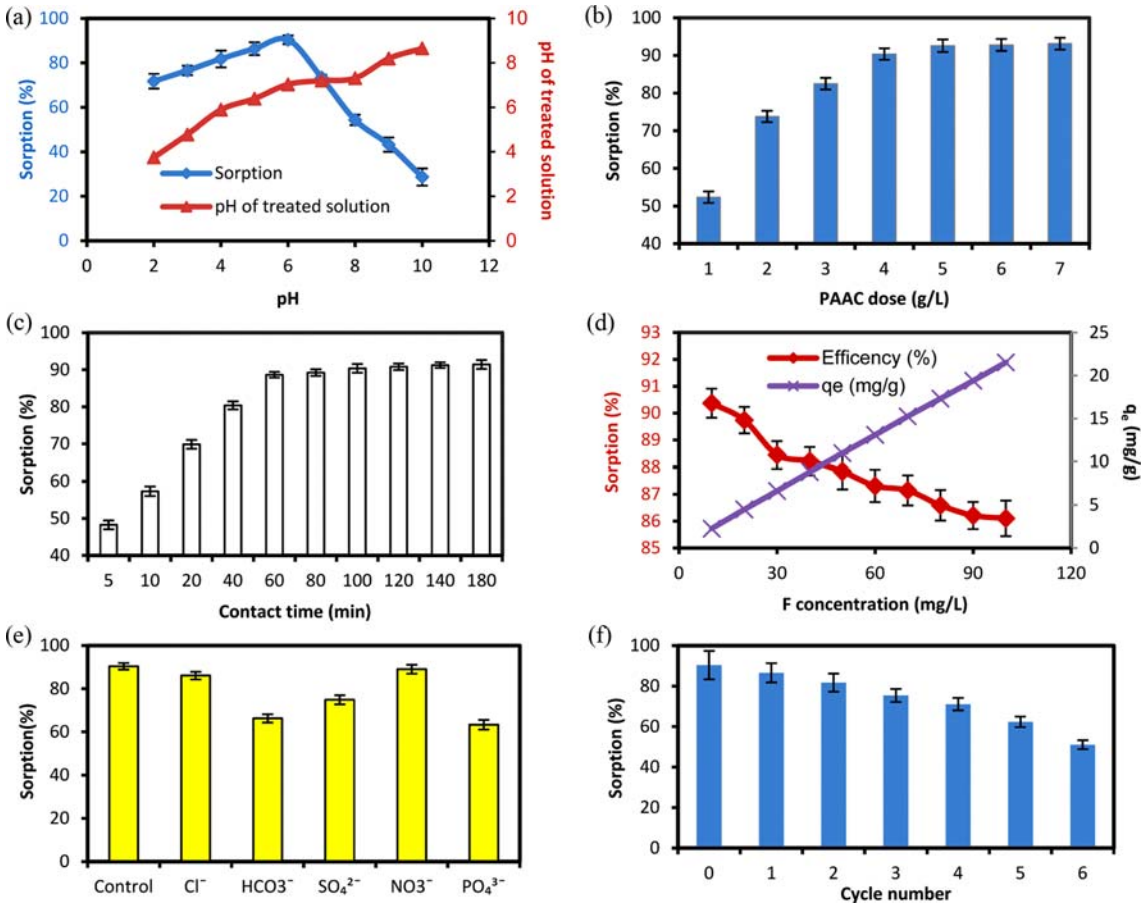

Fig. 4. Effect of (a) pH, PAAC dose, (c) contact time, (d) fluoride concentration, (e) co-existing anions, and (f) reusability of the sorbent.

and O in the activated carbon were observed 87.42% and 12.52%, respectively. The fluoride element is absent in the fresh sorbent. The elements on PAAC were distributed uniformly. Therefore, it can result that the activated carbon produced from the *P. alba* tree has been successfully synthesized. After the adsorption of fluoride ions, the number of pores on the PACC surface was significantly

reduced. This could be due to the presence of fluoride ions (F^-) on the sorbent surface (Fig. 3(d)). The EDX and Map analysis revealed the presence of fluoride ion on the surface of PAAC (Fig. 3(e), (f)), indicating that the activated carbon had a good ability toward F^- adsorption. Note that after the sorption of fluoride ions, the percentage of elements in the activated carbon was altered, which could be due to the reaction of the activated carbon content with fluoride ions [31].

2. Effects of Parameters

The pH of solutions is one of the significant factors that plays a major role in fluoride adsorption. The results of the pH effect investigation are described in Fig. 4(a). A significant difference was detected between the removal efficiency of fluoride in the studied pH range. The results represent that the removal efficiency of fluoride grows along with the increase in the pH from 2 to 6 and then decreases gradually up to 10. The maximum removal rate was observed at a pH of 6. In the acidic condition (pH<6), relatively low F^- removal was seen. The formation of hydrofluoric acid which weakly ionized may be restricted the fluoride ions adsorption [22]. The sharp decrease in removal efficiency under alkaline condition may be due to the competition of the hydroxyl ions (OH^-) with the fluoride ions for adsorption. Similar results for the effect of pH on the fluoride adsorption were explained by Pongener et al. [1], Dehghani et al. [29], and Araga et al. [7]. Fig. 4 also demonstrates the values of pH after the sorption process of fluoride by PAAC. As can be seen, at pH 6, which had the highest adsorption efficiency, the pH value of the treated solution was achieved to be 7.03. Therefore, if this adsorbent is practically applied in the field, there is no need to neutralize the pH of the treated wastewater. As a result, the cost of wastewater treatment will be generally reduced. Also, the increase in solution pH after sorption process confirms the amphoteric property of adsorbent [32].

The effect of sorbent mass on the fluoride removal was considered and the results are depicted in Fig. 4(b). Based on the results, by increasing the PAAC dose from 1 to 4 g/L, the percentage of defluoridation increased and after that, it remained constant. The increase and constant of defloridation percentage can be attributed to increasing the available surface area for adsorbing and sorbent aggregation (which consequently reducing the surface area) [33]. The optimum doses for sorbents of activated bagasse carbon (10 g/L) [34] and *Musa paradisiaca* activated carbon (96 g/L) [10] were more than current research, while that of in the *Manihot esculenta* biomass activated carbon (1.5 mg/L) [1] and *Aegle marmelos* activated carbon (2 g/L) [22] were less than our optimum dose (4 g/L).

Fig. 4(c) displays the percentage of fluoride sorption by PAAC at different contact times. The removal efficiency of fluoride increased rapidly from 5 to 60 min due to the availability of more active sites on the PAAC surface. From 60 to 100 min contact time, the removal of fluoride increased at a very low rate. After 100 min contact time, the defluorination percentage remained constant, which is probably related to the saturation of adsorbent site on the outer interface of the sorbent [31]. Thus, the optimum contact time for defluorination by PAAC was considered to be 100 min. The initial fast removal may be due to the contribution of specific functional groups in the sorption process [22]. Singh et al. [22] reported the ability of bael (*Aegle marmelos*) shell activated carbon to remove 52% of fluoride during 60 min. Based on Suneetha et al. [31], the highest fluoride removal using the *Vitex negundo* activated carbon was obtained as 92% at the contact time of 50 min.

Fig. 4(d) shows the effect of the initial concentration of fluoride (10-100 mg/L) on its removal efficiency using PAAC. The highest (90.37%) and lowest (86.10%) removal rates were observed for fluoride concentrations of 10 and 100 mg/L, respectively. Higher sorption rate at lower initial F^- content is due to the higher ratio of 'surface area to F^- ions', which leads to the use of more energetically active sites on the PAAC adsorbent surface. The plausible reason for the sharp decrease of adsorption efficiency with the increase in the initial F^- content is lack of the sufficient surface area to accommodate more F^- available in the aqueous solution [34]. On the other hand, the adsorption capacity increases with the increase in fluoride concentration. With increasing the initial fluoride concentration from 10 to 100 mg/L, the amount of fluoride adsorbed increased from 2.25 to 21.52 mg/g. The amount of fluoride adsorbed enhances with increasing its initial concentration, *i.e.*, the increase in sorption is limited with PAAC dose. This phenomenon may be due to the increase in the driving force of the concentration gradient with the increase of the initial F^- content. Thus, a higher initial concentration of fluoride will increase the sorption capacity [22].

3. Effect of Co-existing Anions

Fig. 4(e) shows the effect of competing anions on the fluoride sorption by PAAC. The impact of co-existing anions (chloride, nitrate, bicarbonate, sulfate, and phosphate) on the fluoride sorption was assessed. In this research, the mentioned anions were selected as an interfering agent in the sorption of fluoride by PAAC due to the abundance in water and wastewaters [31]. The removal efficiency of fluoride obtained was 89.02%, 86.09%, 74.89%, 66.25%, and 63.38%, in the presence of nitrate, chloride, sulfate, bicarbonate, and phosphate, respectively. Accordingly, nitrate and phosphate had the maximum and minimum effect on F^- removal by PAAC. The order of co-existing anions on the removal efficiency of defluorination is as follows:

Nitrate>Chloride>Sulphate>Bicarbonate>Phosphate

Based on the Sivasankar et al. study, Cl^- and NO_3^- ions constitute the outer sphere surface structure, while SO_4^{2-} ions constitute both the outer and inner-sphere surface structure [35]. Therefore, Cl^- ions and NO_3^- ions have less effect on fluoride removal, while sulfate ions have considerable impacts on defluorination. The bicarbonate ions, which form alkalinity of the water, are the most significant parameter affecting the removal efficiency of fluoride. Bicarbonate ions can reduce the positive charge on the PAAC adsorbent surface and hence cause reducing the affinity of fluoride onto the active sites of the adsorbent [31]. This led to a decrease in the removal efficiency of the F^- ion from aqueous media. The phosphate ions have a higher negative charge than other studied anions and are adsorbed onto PAAC as inner-sphere surface complex [31,36]. Thus, phosphate ions can notably interfere with the F^- ion and decrease the fluoride removal percentage from water.

4. Reusability of the PAAC Sorbent

The major economic and environmental property of an adsorbent is its reusability potential. As depicted in Fig. 4(f), the removal efficiencies of fluoride from the first cycle up to the sixth cycle were

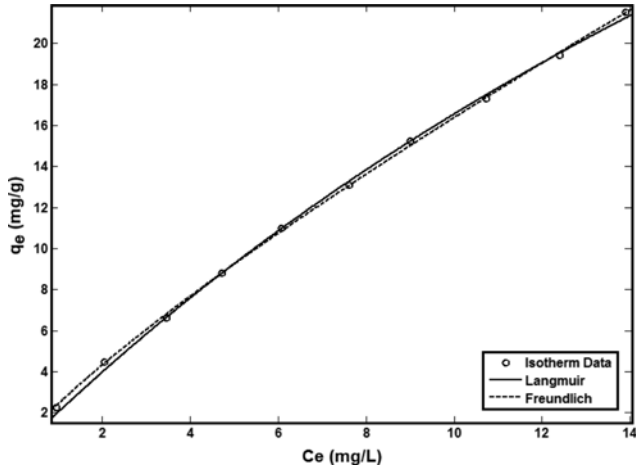

Fig. 5. Isotherm fits for the adsorption of fluoride onto PAAC.

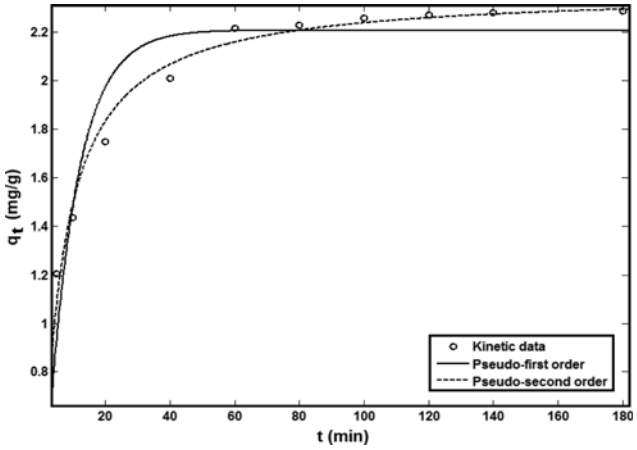

Fig. 6. Kinetic fits for the adsorption of fluoride onto PAAC.

varied from 86.58% to 51.05%, respectively. Results indicated that PAAC can be used several times for the removal of fluoride from aqueous solutions. Based on previous research, different adsorbents, including powdered biochar of *Conocarpus erectus* [33], activated carbon synthesized from *Manihot esculenta* biomass [1], and activated carbon obtained from KOH-treated jamun (*Syzygium cumini*) seed [7], preserved their adsorption capability after seven, three, and one cycles, respectively.

5. Sorption Isotherms

Fig. 5 exhibits the sorption isotherms for defluoridation of an aqueous solution using PAAC. To do this, the most famous isotherm models (Langmuir and Freundlich) were used. The results of the isotherm study are presented in Table 2. As shown, the Freundlich isotherm (highest R^2 value and lowest SSE and RMSE) better described the experimental data for fluoride removal by PAAC than the Langmuir isotherm model. The Langmuir maximum sorption capacity of PAAC was obtained to be 77.12 mg/g, which was higher than the other research works [1,7,14]. Thus, the dependence of sorption data to Freundlich isotherm confirms that the adsorption mechanism is mainly due to being multi-layer and heterogeneous. The result is in agreement with the fluoride removal by other adsorbents like activated alumina, alum and brick powder [37] and natural clay (kaolinite) [38].

In another part of the work, the sorption capacity of ultrasonic-assisted synthesis PAAC was compared with the simple one (non-ultrasonic-assisted). The isotherm test conditions for non-ultrasonic-assisted PAAC were identical to ultrasonic-assisted one. The amount of sorption capacity of non-ultrasonic-assisted PAAC was obtained as 61.77 mg/g. So, it shows that the use of ultrasonic waves can increase the sorption capacity by ≈1.2-times that of non-ultrasonic-assisted PAAC. Accordingly, using ultrasonic waves during the synthesis of the activated carbon adsorbent can be a promising and effective technique.

6. Sorption Kinetics

The models of pseudo-first-order and pseudo-second-order were used to investigate the kinetic manner of the fluoride sorption process (Fig. 6). The parameters of the kinetic model and determination coefficients (R^2) are presented in Table 3. Based on the obtained results, R^2 values for pseudo-first-order and pseudo-second-order kinetics were 0.8797 and 0.9772, respectively, offering that the sorption process of fluoride follows the pseudo-second-order model. The lower error (SSE and RMSE) value also confirms the compatibility of the data with the pseudo-second-order model. Similar results

Table 2. Isotherm results on removal of fluoride by PAAC

Isotherm models	Parameters	R^2	SSE	RMSE
Langmuir	q_m=77.12 mg/g K_L=0.02734 L/mg	0.9989	0.4058	0.2252
Freundlich	K_F=2.451 (mg/g)(L/mg)$^{(1/n)}$ n=1.212	0.9996	0.1572	0.1402

Table 3. Kinetic results on removal of fluoride by PAAC

Kinetic models	Parameters	R^2	SSE	RMSE
Pseudo-first order	k_1=0.1121 min^{-1} $q_{e,cal}$=2.207 mg/g	0.8797	0.1703	0.1459
Pseudo-second order	k_2=0.07229 g/mg/min $q_{e,cal}$=2.368 mg/g	0.9772	0.0322	0.0634

Table 4. Thermodynamics parameters for fluoride sorption onto PAAC

T (K)	ΔG^o (kJ/mol)	ΔH^o (J/mol)	ΔS^o (J/mol·K)
298.15	−4.20	−22.79	−61.69
308.15	−4.01		
318.15	−3.34		
328.15	−2.33		

have been reported by other researchers for fluoride sorption [39,40].

7. Sorption Thermodynamics

Table 4 displays thermodynamics parameters for fluoride adsorption onto PAAC. The value of ΔG^o for the fluoride sorption at various temperatures varied between −2.33 kJ/mol and −4.20 kJ/mol. The negative value of ΔG^o indicated the favorable and spontaneous nature of the adsorption process [41]. Values of ΔH^o and ΔS^o at the temperature ranging from 298.15 K to 328.15 K were −22.79 J/mol and −61.62 J/mol/K, respectively. The negative ΔH^o value shows that the fluoride sorption is exothermic and the negative ΔS^o value indicates the decrease in randomness [42].

8. Field Studies

Table 5 illustrates the treatment of two real samples using *P. alba* activated carbon. In this study, two types of wastewater from the glass and shipyard industries were treated by using PAAC. For both samples, the parameters of pH, BOD_5, COD, F, Ni, Co, and Pb were checked. Results reported that PAAC can significantly remove BOD_5, COD, Ni, Co, Pb, and F. From Table 5, the removal efficiencies of BOD_5, COD, F, Ni, Co, and Pb from glass wastewater were 11.05, 23.25, 66.11, 44.51, 79.83, and ≈100%, respectively, and those for the shipyard wastewater were 8.11, 25.94, 65.45, 48.50, 52.76, and 71.92%, respectively. Based on the results, the pH value of the treatment wastewaters was slightly increased due to replacing fluoride with hydroxyl (OH^-) on the surface of PAAC [4].

CONCLUSIONS

Populus alba activated carbon (PAAC) was synthesized with assisting of ultrasonic waves and used to adsorb fluoride. The sorbent properties were determined using the technique of BET, EDX, XRD, FTIR, SEM, and Map. The specific surface area and pore volume of the PAAC sorbent were obtained as 707.39 m^2/g and 0.40 m^3/g. The results indicate that the maximum removal efficiency of fluoride (93.37%) occurred at conditions of fluoride content of 10 mg/L, PAAC dose of 4 g/L, pH of 6, and contact time of 100 min. The adsorption process data were well fitted with the Freundlich model. Also, the present research data were suitably fitted by the pseudo-second-order kinetic model. The negative value of ΔG^o indicates the favorable and spontaneous nature of the adsorption process. The negative values of ΔH^o and ΔS^o show the fluoride adsorption was exothermic and decrease in randomness respectively. The results show that PAAC sorbent, in addition to efficient fluoride removal, can reduce the parameters of BOD_5, COD, Ni, Co, and Pb of two samples of wastewater to some extent.

REFERENCES

1. C. Pongener, P. C. Bhomick, A. Supong, M. Baruah, U. B. Sinha and D. Sinha, *J. Environ. Chem. Eng.*, **6**, 2382 (2018).
2. G. Asgari, A. Dayari, M. Ghasemi, A. Seid-mohammadi, V. K. Gupta and S. Agarwal, *J. Mol. Liq.*, **275**, 251 (2019).
3. N. Habibi, P. Rouhi and B. Ramavandi, *Environ. Prog. Sustain. Energy*, **38**, S298 (2019).
4. J. P. Maity, C.-M. Hsu, T.-J. Lin, W.-C. Lee, P. Bhattacharya, J. Bundschuh and C.-Y. Chen, *Environ. Nanotech. Monit. Manag.*, **9**, 18 (2018).
5. J. Singh, P. Singh and A. Singh, *Arabian J. Chemist.*, **9**, 815 (2016).
6. M. Davodi, H. Alidadi, A. Ramezani, B. F. Jamali and Z. Bonyadi, *Desal. Water Treat.*, **137**, 292 (2019).
7. R. Araga, S. Soni and C. S. Sharma, *J. Environ. Chem. Eng.*, **5**, 5608 (2017).
8. C. Janardhana, G. N. Rao, R. S. Sathish and V. S. Lakshman, *Indian J. Chem. Technol.*, **13**, 414 (2006).
9. C. Chakrapani, C. Babu, K. Vani and K. S. Rao, *J. Chemist.*, **7**, S419 (2010).

Table 5. Treatment of two real samples using PAAC

Wastewater type	Factor	Unit	Raw	Treated
Glass wastewater	pH	Unit of pH	6.30±0.27	6.68±0.09
	BOD_5	mg/L	208.19±3.11	185.27±2.1
	COD	mg/L	129±5.91	99.1±3.29
	F	mg/L	24.38±0.15	8.26±0.18
	Ni	mg/L	10.02±0.31	5.56±0.51
	Co	mg/L	4.81±0.13	0.97±0.15
	Pb	mg/L	2.08±0.98	No-detectable
Shipyard wastewater	pH	Unit of pH	6.35±0.3	6.89±0.21
	BOD_5	mg/L	258.9±1.92	237.9±2.03
	COD	mg/L	173±0.93	128.11±1.87
	F	mg/L	11±0.71	3.8±0.55
	Ni	mg/L	12±0.71	6.18±0.28
	Co	mg/L	13±0.71	6.14±0.27
	Pb	mg/L	14±0.71	3.93±0.67

10. T. Getachew, A. Hussen and V. M. Rao, *Int. J. Environ. Sci. Technol.*, **12**, 1857 (2015).
11. G. Alagumuthu, V. Veeraputhiran and R. Venkataraman, *Hemijska Industrija*, **65**, 23 (2011).
12. D. Mehta, P. Mondal, V. K. Saharan and S. George, *Ultrason. Sonochem.*, **40**, 664 (2018).
13. M. S. Samuel, V. Subramaniyan, J. Bhattacharya, R. Chidambaram, T. Qureshi and N. P. Singh, *Ultrason. Sonochem.*, **48**, 412 (2018).
14. A. Mullick and S. Neogi, *Ultrason. Sonochem.*, **50**, 126 (2019).
15. A. Mullick and S. Neogi, *Ultrason. Sonochem.*, **45**, 65 (2018).
16. B. S. Al-Farhan, *J. Environ. Analyt. Toxicol.*, **5**, 1 (2014).
17. H. Sixto, B. D. González-González, J. J. Molina-Rueda, A. Garrido-Aranda, M. M. Sanchez, G. López, F. Gallardo, I. Cañellas, F. Mounet and J. Grima-Pettenati, *Trees*, **30**, 1873 (2016).
18. R. Martín-Sampedro, J. I. Santos, Ú. Fillat, B. Wicklein, M. E. Eugenio and D. Ibarra, *Int. J. Biolog. Macromol.*, **126**, 18 (2019).
19. M. Shahverdi, E. Kouhgardi and B. Ramavandi, *Data in Brief*, **9**, 163 (2016).
20. B. Heibati, S. Rodriguez-Couto, M. A. Al-Ghouti, M. Asif, I. Tyagi, S. Agarwal and V. K. Gupta, *J. Mol. Liq.*, **208**, 99 (2015).
21. H. Hossaini, G. Moussavi and M. Farrokhi, *Water Res.*, **59**, 130 (2014).
22. K. Singh, D. H. Lataye and K. L. Wasewar, *J. Fluor. Chem.*, **194**, 23 (2017).
23. A. Supong, P. C. Bhomick, M. Baruah, C. Pongener, U. B. Sinha and D. Sinha, *Sustain Chem. Pharm.*, **13**, 100159 (2019).
24. R. Foroutan, R. Mohammadi, J. Razeghi and B. Ramavandi, *Algal Res.*, **40**, 101509 (2019).
25. R. Foroutan, M. Ahmadlouydarab, B. Ramavandi and R. Mohammadi, *J. Environ. Chem. Eng.*, **6**, 6049 (2018).
26. R. Foroutan, R. Zareipour and R. Mohammadi, *Mater. Res. Exp.*, **6**, 025508 (2018).
27. R. K. Bharali and K. G. Bhattacharyya, *J. Environ. Chem. Eng.*, **3**, 662 (2015).
28. Z. Esvandi, R. Foroutan, M. Mirjalili, G. A. Sorial and B. Ramavandi, *J. Polym. Environ.*, **27**, 263 (2019).
29. M. H. Dehghani, M. Farhang, M. Alimohammadi, M. Afsharnia and G. Mckay, *Chem. Eng. Commun.*, **205**, 955 (2018).
30. S. Raghav, S. Nehra and D. Kumar, *J. Mol. Liq.*, **284**, 203 (2019).
31. M. Suneetha, B. S. Sundar and K. Ravindhranath, *J. Analyt. Sci. Technol.*, **6**, 15 (2015).
32. B. Ramavandi and G. Asgari, *Process Saf. Environ.*, **116**, 61 (2018).
33. F. Papari, P. R. Najafabadi and B. Ramavandi, *Desal. Water Treat.*, **65**, 375 (2017).
34. A. K. Yadav, R. Abbassi, A. Gupta and M. Dadashzadeh, *Ecolog. Eng.*, **52**, 211 (2013).
35. V. Sivasankar, S. Rajkumar, S. Murugesh and A. Darchen, *Chem. Eng. J.*, **197**, 162 (2012).
36. L. Delgadillo-Velasco, V. Hernández-Montoya, N. A. Rangel-Vázquez, F. J. Cervantes, M. A. Montes-Morán and M. d. R. Moreno-Virgen, *J. Mol. Liq.*, **262**, 443 (2018).
37. K. U. Ahamad, R. Singh, I. Baruah, H. Choudhury and M. R. Sharma, *Groundw Sustain Dev.*, **7**, 452 (2018).
38. N. Nabbou, M. Belhachemi, M. Boumelik, T. Merzougui, D. Lahcene, Y. Harek, A. A. Zorpas and M. Jeguirim, *C. R. Chim.*, **22**, 105 (2019).
39. K.-Y. A. Lin, Y.-T. Liu and S.-Y. Chen, *J. Colloid Interface Sci.*, **461**, 79 (2016).
40. M. H. Dehghani, G. A. Haghighat, K. Yetilmezsoy, G. McKay, B. Heibati, I. Tyagi, S. Agarwal and V. K. Gupta, *J. Mol. Liq.*, **216**, 401 (2016).
41. Z. A. Al-Othman, M. A. Habila, R. Ali and M. S. E.-d. Hassouna, *Asian J. Chemist.*, **25**, 8301 (2013).
42. M. Danish, T. Ahmad, S. Majeed, M. Ahmad, L. Ziyang, Z. Pin and S. S. Iqubal, *Bioresour. Technol. Rep.*, **3**, 127 (2018).